INCLUSIVE PUBLISHING TRUSTED SCIENCE
PURPOSE-LED PUBLISHING™

PAPER • **OPEN ACCESS**

Sustainable synthesis of silver oxide nanoparticles from *Lobularia maritima*: a new approach to antioxidant and photocatalytic applications

To cite this article: Uma Koul *et al* 2025 *Nano Ex.* **6** 045016

View the article online for updates and enhancements.

You may also like

- Shape-controlled synthesis of Cu_2O nanoparticles with single-digit nanoscale void space via ionic liquid/metal sputtering and their photoelectrochemical properties
Shushi Suzuki, Atsumi Morimoto, Susumu Kuwabata et al.

- Photoelectrochemical and Non-Enzymatic Glucose Sensor Based on Modified Fehling's Test by Using Ti/TiO_2 NTs-rGO-Cu_2O Electrode
Bekir Çakrolu and Mahmut Özacar

- Mechanism of strong visible light photocatalysis by Ag_2O-nanoparticle-decorated monoclinic TiO_2(B) porous nanorods
Kamal Kumar Paul, Ramesh Ghosh and P K Giri

kiutra

Millikelvin characterization for superconducting devices

L-TYPE RAPID

- **< 4 hrs** sample loading and cooldown to base
- **50 mK** base temperature
- **30 min** warm up and sample exchange

Find out more →



This content was downloaded from IP address 217.74.153.144 on 05/10/2026 at 07:48

NANO EXPRESS

Check for updates

OPEN ACCESS

RECEIVED
28 May 2025

REVISED
2 December 2025

ACCEPTED FOR PUBLICATION
15 December 2025

PUBLISHED
24 December 2025

Original content from this work may be used under the terms of the Creative Commons Attribution 4.0 licence.

Any further distribution of this work must maintain attribution to the author(s) and the title of the work, journal citation and DOI.

PAPER

Sustainable synthesis of silver oxide nanoparticles from *Lobularia maritima*: a new approach to antioxidant and photocatalytic applications

Uma Koul[1], **Ruchi Bharti**[1,*], **Renu Sharma**[1], **Ajay Thakur**[1], **Monika Verma**[1] and **Annu Pandey**[2,*]

[1] Department of Chemistry, University Institute of Sciences, Chandigarh University, Mohali, Punjab (140413), India
[2] Department of Fibre and Polymer Technology, KTH Royal Institute of Technology, Stockholm, Sweden
[*] Authors to whom any correspondence should be addressed.

E-mail: ruchi.uis@cumail.in, an-nua@kth.se and annua@kth.se

Keywords: green synthesis, silver oxide nanoparticles, antioxidant activity, *Lobularia maritima*, photo catalytic degradation

Supplementary material for this article is available online

Abstract

This study introduces a green and sustainable method for synthesizing silver oxide nanoparticles (Ag_2O NPs) using *Lobularia maritima* extract as a natural reducing and stabilizing agent. Unlike traditional chemical and physical methods that rely on toxic reagents and high energy inputs, this eco-friendly approach is cost-effective, safer, and aligns with green chemistry principles. The synthesized Ag_2O NPs exhibited impressive antioxidant activity, with $80 \pm 0.02\%$ 2,2′-Azino-bis(3-ethylbenzothiazoline-6-sulfonic acid (ABTS) and $75 \pm 0.02\%$ 2,2-diphenyl-1-picrylhydrazyl (DPPH) scavenging efficiencies, comparable to those of ascorbic and gallic acids. In photocatalytic tests, they achieved 91% degradation of methylene blue under visible light within 120 min, outperforming many chemically synthesized Ag_2O NPs. Characterization via ultraviolet-visible (UV–vis) spectroscopy, Fourier transform infrared (FTIR), scanning electron microscopy with energy dispersive x-ray analysis (SEM-EDX), dynamic light scattering (DLS), and x-ray diffraction (XRD) confirmed the high purity, stability, and controlled morphology of the samples. These findings highlight the potential of plant-based Ag_2O NPs for real-world applications in environmental cleanup and biomedical fields. Future research can focus on scaling production and testing biocompatibility for broader industrial use.

Abbreviations

ABTS	2,2′-Azino-bis(3-ethylbenzothiazoline-6-sulfonic acid)
DPPH	2,2-Diphenyl-1-picrylhydrazyl
TAC	Total Antioxidant Capacity
XRD	X-ray Diffraction
FTIR	Fourier Transform Infrared Spectroscopy
UV–vis	Ultraviolet–Visible Spectroscopy
Ag_2O NP	Silver Oxide Nanoparticles
MB	Methylene Blue
k_1	Pseudo-First-Order Rate Constant
$AgNO_3$	Silver Nitrate
k_2	Pseudo-Second-Order Rate Constant
R^2	Coefficient of Determination
$t_{1/2}$	Half-life

© 2025 The Author(s). Published by IOP Publishing Ltd

ROS	Reactive Oxygen Species
NPs	Nanoparticles

1. Introduction

Recently, silver oxide nanoparticles (Ag_2O NPs) are increasingly becoming a relevant material and possess unique physical characteristics, such as their optical, catalytic, and biological properties, which represent a multitude of possible applications in both environmental remediation and healthcare [1, 2]. Ag_2O NPs have excellent photocatalytic characteristics that allow them to decompose organic pollutants, due to their high surface area and reactive attributes [3]. The unique antimicrobial and antioxidant characteristics of Ag_2O NPs make them useful in many medical-related applications, including wound healing, drug delivery, and coatings on medical devices [4]. Ag_2O NPs can be synthesized by traditional methods of physical or chemical synthesis [5]. The chemical method for producing Ag_2O NPs generally uses the following reducing agents for silver salt production: hydrazine, sodium borohydride, and ascorbic acid. Chemical synthesis allows the formation of Ag_2O NPs with control over the particle size and shape. However, many commercial items such as silver oxide NPs and other types of metallic NPs use chemical synthesis methods to manufacture their products, therefore creating issues regarding the use of hazardous chemicals [6].

Moreover, traditional chemical methods can create serious risks for health and the environment due to toxic and volatile chemical reagents that are used [7]. The disposal of the chemical waste obtained from these methods can negatively impact the environment [8]. Physical methods to produce high-purity nanoparticles consume a large amount of energy and need complex equipment; therefore, they are not as sustainable or economically feasible compared to green synthesis techniques. Both physical and chemical methods can only be used in resource-limited environments with access to energy and infrastructure, thus demonstrating the need for more environmentally-friendly and easily accessible production methods [9, 10]. Green synthesis has emerged as an alternative solution to the limitations of the above methods; using natural resources like plant extracts, bacteria, fungi and algae to reduce silver ions has been identified as a new method to produce silver nanoparticles [11]. The additional benefit of using the natural phytochemicals contained within plants for both reducing and stabilising agents eliminates the need for additional toxic reagents, reducing the environmental impact of silver nanoparticle production [12, 13]. Many different plants have already been investigated using green synthesis technology, including *Parieteria alsinaefolia* [14] *Croton macrotachyus* [15], and Mistletoe [16], which have demonstrated the potential to synthesize biocompatible Ag_2O NPs with valuable bioactivities, and more literature can be studied in table S1 (please see the supporting information (SI)). It is easier, less poisonous, cheaper, and adheres to green chemistry principles [17].

Furthermore, plant extracts also contain natural capping agents that enhance the stability and functionality of Ag_2O NPs, which are required for applications involving biocompatibility, such as in biomedical and environmental fields [18]. However, green synthesis can sometimes result in a broader particle size distribution, and the degree of purity may be less than that achieved through physical methods [19]. Despite these potential limitations, advancements in optimizing green protocols improve nanoparticle quality, making this approach increasingly feasible for diverse applications [20].

As part of broader efforts in sustainable nanotechnology [21–26], this study presents an environmentally benign strategy for synthesizing Ag_2O nanoparticles using *Lobularia maritima* extract. The resulting nanoparticles were thoroughly characterized to evaluate their structural, morphological, and functional properties, demonstrating considerable promise for environmental and biomedical applications

We present a method of synthesizing silver oxide nanoparticles (Ag_2O NPs) using a green process that can easily be scaled up to meet production demand. The work done here demonstrates how these nanoparticles can help solve major global challenges such as pollution and providing healthcare products, like antioxidant supplements, for sustainability in science and technology.

2. Experimental procedures

2.1. Collection and preparation of the plant extract

For the green synthesis of silver oxide nanoparticles, *Lobularia maritima* was selected due to its medicinal value and the abundance of bioactive compounds that can serve as natural reducing and stabilizing agents. Fresh plant material was collected from the Punjab region, thoroughly washed with tap water, and finally rinsed with distilled water to remove any surface impurities. After drying, 10 grams of the plant material were added to a 250 ml conical flask containing 100 ml of ethanol. The mixture was heated at 50 °C for 10 min with gentle

stirring to extract the bioactive compounds. Once the extraction was complete, the solution was filtered through Whatman no. 1 filter paper, and the resulting clear filtrate was set aside for the nanoparticle synthesis.

2.2. Synthesis of Ag_2O-NPs

The method for synthesizing Ag_2O nanoparticles is much the same as that described above for Ag metallic nanoparticles except that the product formed from the above description will be Ag_2O, rather than Ag. Similarly, the color of the solution during synthesis was green to dark blackish grey, with centrifugation occurring after about two hours at 3000 rpm, allowing the solid particles to settle out of the liquid, which was then removed. The solid obtained was dried in an oven at 40 °C for approximately 12 h, and the Ag_2O NPs were then kept in vials for further characterization and testing, as shown in figure S1 referred SI.

2.3. Characterization of Ag_2O NP

2.3.1. Ultraviolet-visible spectral assay

The antioxidant activity of synthesized Ag_2O-NPs was analyzed through ultraviolet-visible (UV–vis) spectral analysis on a UV-2450 instrument. The wavelength ranged from 200 to 800 nm, and a quartz cuvette with a 1 cm path length was used. This assured an exact measurement of the nanoparticles' antioxidant properties.

2.3.2. FTIR spectral analysis

FTIR analysis was performed using a PerkinElmer Spectrum Two instrument to investigate the presence of functional groups in both the plant extract and synthesized Ag_2O-NPs. The FT-IR spectrum was measured in the range of 400–4000 cm^{-1}.

2.3.3. SEM -EDX analysis

Scanning Electron Microscopy (SEM) was performed using the JSM IT500 microscope, equipped with a secondary electron (SE) detector for imaging and an energy-dispersive x-ray (EDX) detector for elemental analysis. The samples were coated with a thin layer of gold using a sputter coater to facilitate conductivity and eliminate charging effects before imaging. Using a spin coater at 3000 RPM for 30 seconds, thin film samples were prepared by applying uniform samples to glass slides. After applying the sample, they were dried under an infrared lamp at approximately 60 degrees Celsius for five minutes to remove any remaining water before starting SEM preparation. The SEM-EDX provided information about the elemental composition and distribution of the components within the nanoparticles using EDX.

2.3.4. Dynamic light scattering (DLS)

The particle size distribution of Ag_2O-NPs synthesised was evaluated with Mastersizer 3000 (DLS) as it provides an accurate particle size distribution of the particles present.

2.3.5. XRD analysis

Using a Bruker D8 Advance x-ray Diffraction Ab (XRD) analysis was performed to evaluate the phase purity and crystal structure of Ag2O nanoparticles. The XRD machine used Cu Kα radiation ($\lambda = 1.54$ Å) to scan from 20° to 90°, at a speed of 0.05° per minute, with a time constant of 2 s. These results are similar to those in JCPDS Card number 84-1108 and confirm that silver oxide is crystalline [1].

3. Result and discussion

Lobularia maritima was used to prepare silver oxide (Ag_2O) nanoparticles, as outlined in the Experimental Procedures section. To characterise the nanoparticles, ultra-violet/visible (UV–vis), Fourier transform infrared (FTIR), scanning electron microscopy (SEM), dynamic laser diffraction (DLS), and x-ray diffraction (XRD) methods were used. These analyses demonstrated successful formation of Ag_2O NPs, their intended morphology, and their crystalline structure. Below we discuss the characteristics of the NPs, and their performance.

3.1. Optimization of synthesis parameters for Ag_2O Nps

To optimise the preparation of silver oxide nanoparticles, various synthesis parameters were analysed such as the ratio of plant extract to silver precursor, concentration of silver precursor, and pH (figure 1). The influence of these parameters on the particle properties was also evaluated to determine the ideal conditions that promote practical synthesis, stabilization, and uniformity of Ag_2O NPs. These parameters were selected based on their Influence on the nanoparticle size, stability, and yield. Adjusting these variables enabled us to identify

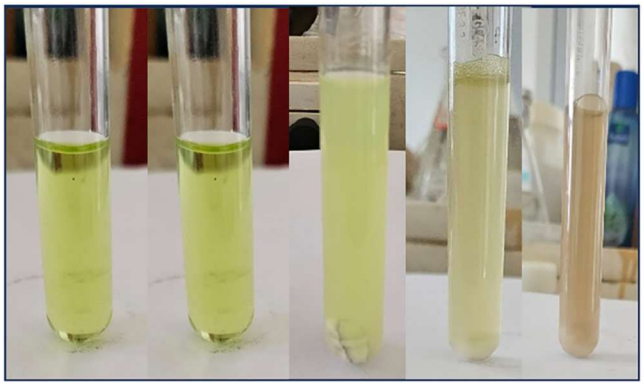


Figure 1. Optimization of synthesis parameters for green-synthesized Ag_2O nanoparticles.

conditions that optimize the reduction of silver ions, allowing us to produce Ag_2O NPs with desirable properties for potential applications.

3.1.1. Effect of plant extract on metal precursor ratio

The plant extract-to-metal precursor ratio is relevant in balancing phytochemicals with metal ions, which directly influences the reduction reaction and stability of the nanoparticles. We considered several ratios—1:4, 2:3, 3:2, and 4:1—and based on the successful reduction, we observed a color change from green to brown in the obtained solution. A 1:1 ratio produced the best between these, as witnessed by an absorption peak at 290 nm, as shown in figure 2(a). This ratio provided an efficient balance, allowing the bioactive compounds in the plant extract to effectively reduce and stabilize the silver ions, resulting in the formation of silver nanoparticles with well-defined features. The appearance of the peak at 290 nm indicates that this ratio enhances particle formation effectively while minimizing excess reagents.

3.1.2. Influence of silver precursor concentration

The concentration of the silver precursor ($AgNO_3$) was varied to assess its effect on nanoparticle yield and size. Through the use of concentrations of 0.1 M, 0.2 M, 0.3 M, 0.4 M, and 0.5 M, we found that a concentration of 0.1 M produced a strong absorbance peak at 290 nm (figure 2(b)). The higher concentrations of silver ions was observed to increase the speed of reduction, but high concentrations induced particle aggregation, which is known to affect nanoparticle stability. Therefore, an optimal concentration of 0.1 M was achieved, resulting in effective nanoparticle formation within the colloidal stability range.

3.1.3. Influence of pH on nanoparticle synthesis

The reaction environment's pH significantly influences the reduction process, stability, and surface charge of the synthesized nanoparticles. We tested the synthesis at acidic, neutral, and basic pH values. The best results were obtained at a neutral pH, with an absorbance peak at 300 nm (figure 2(c)), indicating the formation of stable and well-dispersed nanoparticles. At a neutral pH, the reduction of silver ions is optimized, providing a stable environment that enhances nanoparticle formation and prevents unwanted agglomeration.

3.2. Characterization techniques

3.2.1. FT-IR spectral assay

The FTIR spectra of the *Lobularia maritima* plant extract and the synthesized Ag_2O nanoparticles (figure 3) provide key information about the functional groups involved in reducing Ag^+ ions and stabilizing the formed nanoparticles.

A characteristic peak due to hydroxyl (O–H), carbonyl (C=O), aliphatic C–H, and C–O functional groups is seen in the plant extract spectrum. These functional groups are commonly found in biomolecules, such as phenolics, flavonoids, terpenoids, and proteins, which can all serve as natural reducing and capping agents [10].

Upon nanoparticle formation, the FTIR spectrum of Ag_2O NPs exhibits shifts and changes in intensity of various prominent peaks, indicating the interaction of plant-derived functional groups with the nanoparticle surface. Further, Ag–O bond-related new peaks at the low-wavenumber region (542–715 cm^1) confirm the practical synthesis of Ag_2O NPs.

The shifts in O–H and C=O stretching frequencies, as well as C–O and C–N vibrations, provide strong evidence that the phytochemicals in the plant extract play an active role in reducing Ag^+ ions and stabilizing

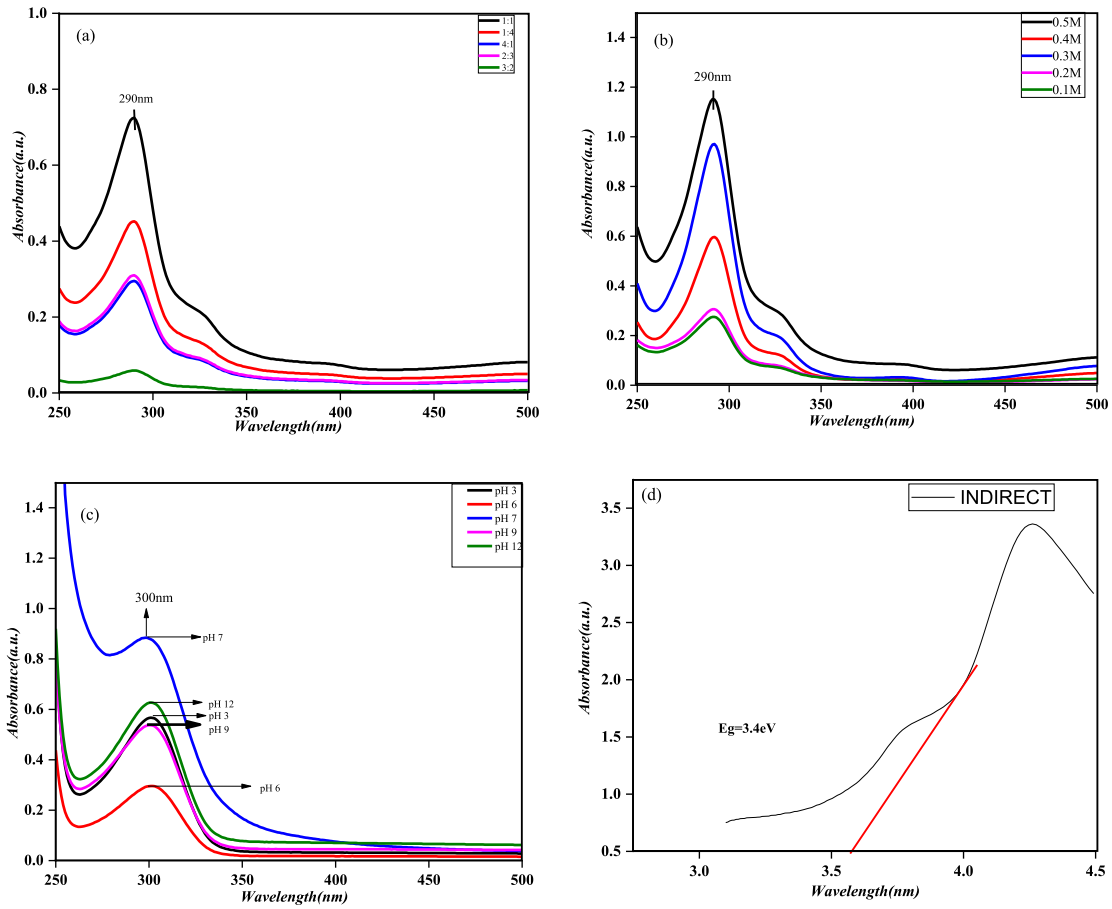


Figure 2. (a) UV–vis absorbance spectra for various plant extract-to-silver precursor ratios showing the effect on nanoparticle formation. (b) Effect of silver nitrate concentration on nanoparticle synthesis as indicated by changes in absorbance. (c) Influence of reaction pH on absorbance peak and particle stability. (d) Tauc plot used to estimate the optical band gap of synthesized nanoparticles. 4 mg (c) 6 mg (d) 8 mg and (e) 10 mg of 20 ppm solution. 4 mg (c) 6 mg (d) 8 mg and (e) 10 mg of 20 ppm solution. Values represent the mean ± standard deviation (n = 3).

Ag_2O nanoparticles. The newly appeared peaks within the 500–750 cm^{-1} range are indicative of Ag–O vibrations, which evidence the successful formation of silver oxide.

These results are consistent with earlier research [1, 27], which found that green synthesis pathways based on plants exhibit comparable FTIR signatures characteristic of biomolecule–metal interactions and Ag–O bond formation as shown in table 1.

FTIR analysis thereby unambiguously establishes the bifold role of *Lobularia maritima* extract: (i) reduction of silver ions to Ag^0 and Ag_2O, and (ii) stabilization of nanoparticles by surface adsorption of organic functional groups.

3.2.2. Dynamic light scattering (DLS)

Dynamic light scattering (DLS) analysis was employed to determine the size distribution of the Ag_2O nanoparticles. The resulting intensity distribution profile (figure 4) exhibited a prominent, narrowly defined peak at about 43 nm, which is indicative of a highly uniform, monodisperse suspension. The absence of any secondary peaks strongly suggests that there is minimal aggregation and that the population of nanoparticles within the solution is well stabilized.

The 43 nm hydrodynamic diameter includes contributions from the metallic core and the solvation shell surrounding it, in addition to residual biomolecules from the *Lobularia maritima* extraction method. As a result of this method, x-ray diffraction-derived values for crystallite size will typically be less than what is observed via particle size measurement. The PDI value is indicative of a very uniform and stable distribution of the Ag_2O nanoparticles in solution (PDI = 0.21).

In conclusion, results indicate that the green synthesis process produces Ag_2O at high levels of monodispersity and stable distribution, despite a minor amount of variation due to natural variability between plant capping agents. This uniformity is ideal for use in applications requiring consistent-sized and stable nanomaterials.

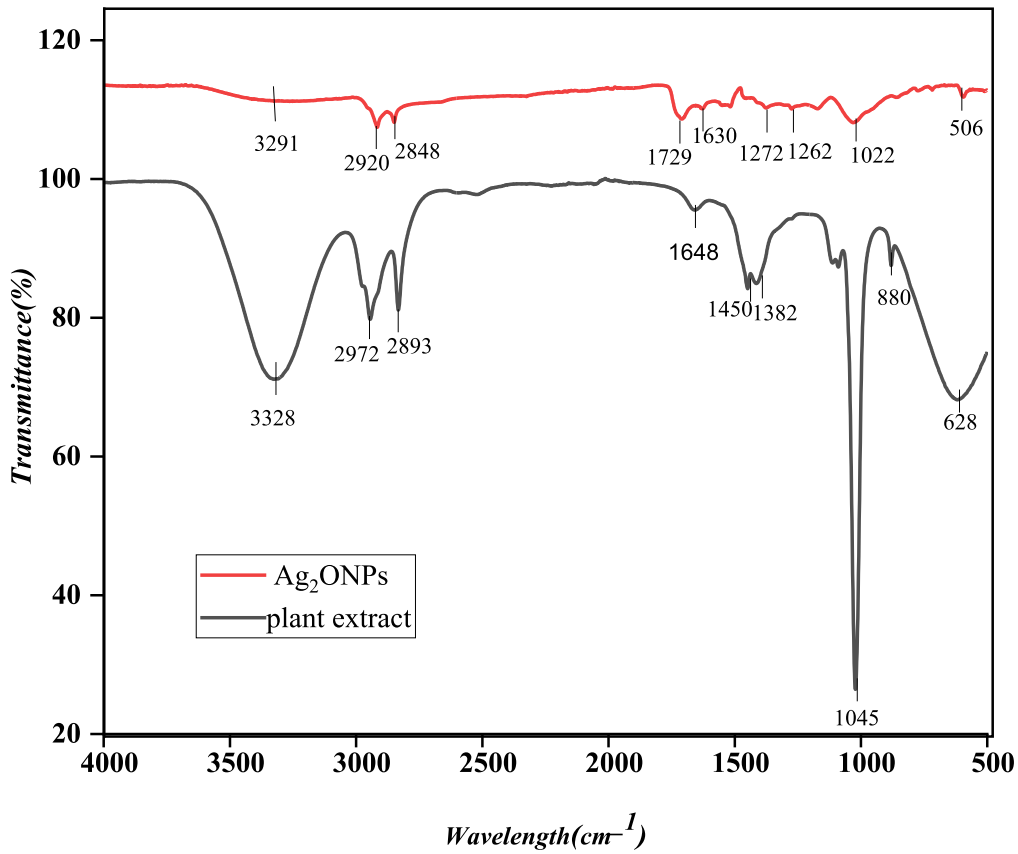


Figure 3. FTIR spectra of plant extract and FTIR spectra of Ag_2O NPs.

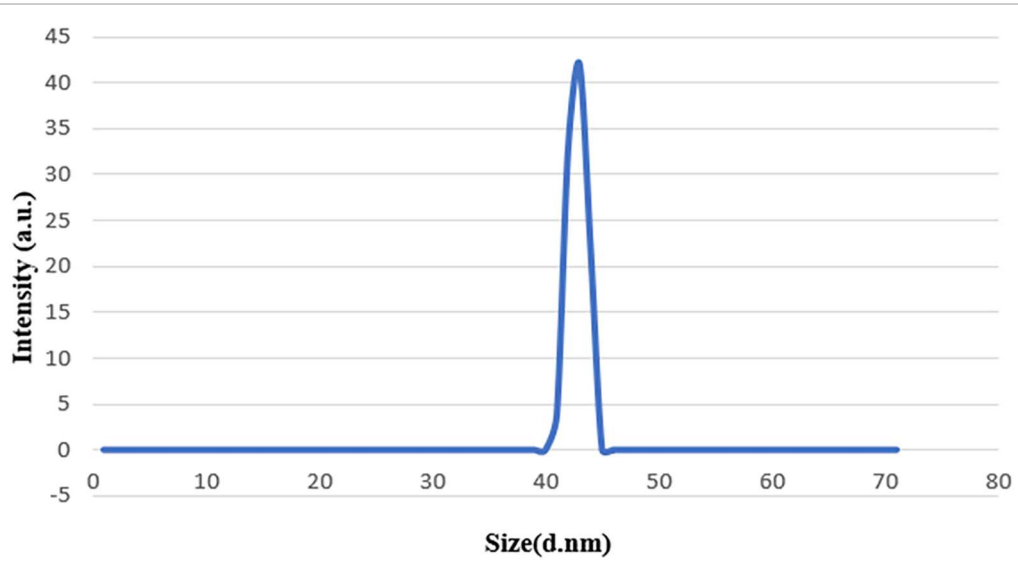


Figure 4. DLS intensity distribution curve of the synthesized Ag_2O nanoparticles.

3.2.3. SEM -EDX analysis of AgNPs

The as synthesized Ag2O particle's microstructure and surface morphology were analysed using SEM imaging (figures 5(a)–(b)). The SEM images exhibit a high degree of crystallinity due to the well-formed angular/faceted structure of the crystal particles, even though there is significant aggregation of the Ag_2O particle's crystals most likely from drying and/or inter particle van der Waals forces which cause the particles to clump together after synthesis. There is enough distinction between the interface of two separate particles for you to see that the particles have a tendency to cluster together.

Table 1. Comparative FTIR analysis of plant extract and synthesized Ag_2O nanoparticle.

Functional group	Plant extract (cm^1)	Ag_2O NPs (cm^1)	Observation	Interpretation
O–H stretching (hydroxyl)	3328	3291	Shifted	Participation in reduction/stabilization
C–H stretching (aliphatic)	2972, 2893	2920, 2848	Shifted	Involvement in capping or organic coating
C=O stretching (carbonyl/ carboxyl)	1648, 1450	1729, 1660	Shifted/upshifted	Coordination with metal ions
C=C aromatic ring	1382, 1322	1630, 1585, 1461	New or shifted	Possible aromatic involvement in binding
C–O stretching (alcohol/ether)	1277, 1082, 1045	1273, 1217, 1167	Slight shift	Role in stabilization
C–N stretching (amines)	1045	1030	Shifted	Interaction with Ag^+ ions
Ag–O stretching	—	715, 591, 542	New peaks	Confirmation of Ag_2O formation

Using ImageJ, more than 20 separate individual particle's sizes were measured from digitised SEM images (figure 5(b)) to quantify the size of particles. The size of Ag_2O crystals measured, ranged from approximately 125 nm–550 nm and had an average particle size of 260 ± 80 nm. These data confirm that the Ag_2O material is comprised of crystalline (sub-micron) particles, with most of the crystallizing particle sizes being greater than conventional nanoparticles (< 100 nm).

The elemental composition was determined using energy-dispersive x-ray spectroscopy (EDX) as depicted in figure 5(a) The EDX spectrum demonstrates that the principal elements present were Ag and O, with the average percentages of $81.81 \pm 1.18\%$ and $18.12 \pm 0.97\%$, respectively. Therefore, this confirms that the compound being analysed is indeed Ag_2O. A trace amount of N ($0.08 \pm 0.48\%$) was also recorded, which is probably due to the presence of small amounts of contamination from the atmosphere and/or other sources, but the amount is negligible. As can be seen in figure 5(a), there are also other very small elements, including, which are most likely linked to contamination or the capping agents used in the synthesis of the Ag_2O materials., as shown in table S2(referred SI).

3.2.4. XRD analysis

Distinct peaks were revealed by x-ray Diffraction (XRD) analysis at specific 2θ angles of 38.2°, 44.3°, 64.5°, and 77.4°. These peaks were associated with the crystalline structure of Ag_2O nanoparticles produced in figure 6. The clear resolution of the diffraction peaks also identifies each of these peaks with a corresponding crystallographic plane; the first peak is attributed to (111), the second peak is from (200), the third peak represents (220), and the fourth peak reflects (311). In addition, there is a positive correlation with the data retrieved from the JCPDS Card# 84-1108, which is a very good indication of the accuracy of the determination of the structure of silver oxide (Ag_2O) being face-centred cubic (FCC) [28]. The average crystallite size was calculated using the Debye–Scherrer equation [29] based on the most intense (111) peak at 38.2°, and was found to be approximately 24.7 nm, confirming the nanocrystalline nature of the particles. Notably, the apparent differences between the size values obtained from XRD, DLS, and Sem are fully consistent when the nature of each technique is considered. The crystallite size of 24.7 nm from XRD reflects the dimension of coherent diffracting domains within the Ag_2O nanocrystals. The hydrodynamic diameter of 43 nm, measured by DLS, is larger because it includes the solvated shell and phytochemical capping layer surrounding the nanocrystalline core in the aqueous dispersion. In contrast, the mean size of 260 ± 80 nm observed in SEM arises from dry-state aggregates formed during sample preparation, where individual nanocrystallites cluster via capillary and Van der Waals forces. Thus, the hierarchy 24.7 nm (XRD), 43 nm (DLS), 260 nm (SEM) supports a model of nanoscale primary crystallites that are colloidally stable in solution but tend to assemble to larger agglomerates upon drying, resolving the apparent discrepancy.

4. Photocatalytic activity of Ag_2O NPS

The synthesized silver oxide nanoparticles (Ag_2O NPs) were tested for their ability to degrade methylene blue (MB) dye with the aid of visible light. The results of this test provided a measure of how effective these materials could be used in an environmentally friendly way to remove contaminants from the environment. Additionally, this experiment confirmed that Ag_2O NPs have the ability to meet the goals of sustainable and green chemistry, including being less expensive and more efficient in removing pollutants from the environment.

The degradation of the MB molecule was measured by using a spectrophotometer to measure the absorbance at 293 nm and at 664 nm (the wavelengths at which the MB molecule absorbs the greatest amount of light), and thus determined the extent to which the MB molecule had broken down during the experiment over time. The decreasing absorbance values shown in figure 7 indicated that the Ag_2O nanoparticles had demonstrated photocatalytic activity in degrading MB. The maximum photodegradative efficiency was recorded at an

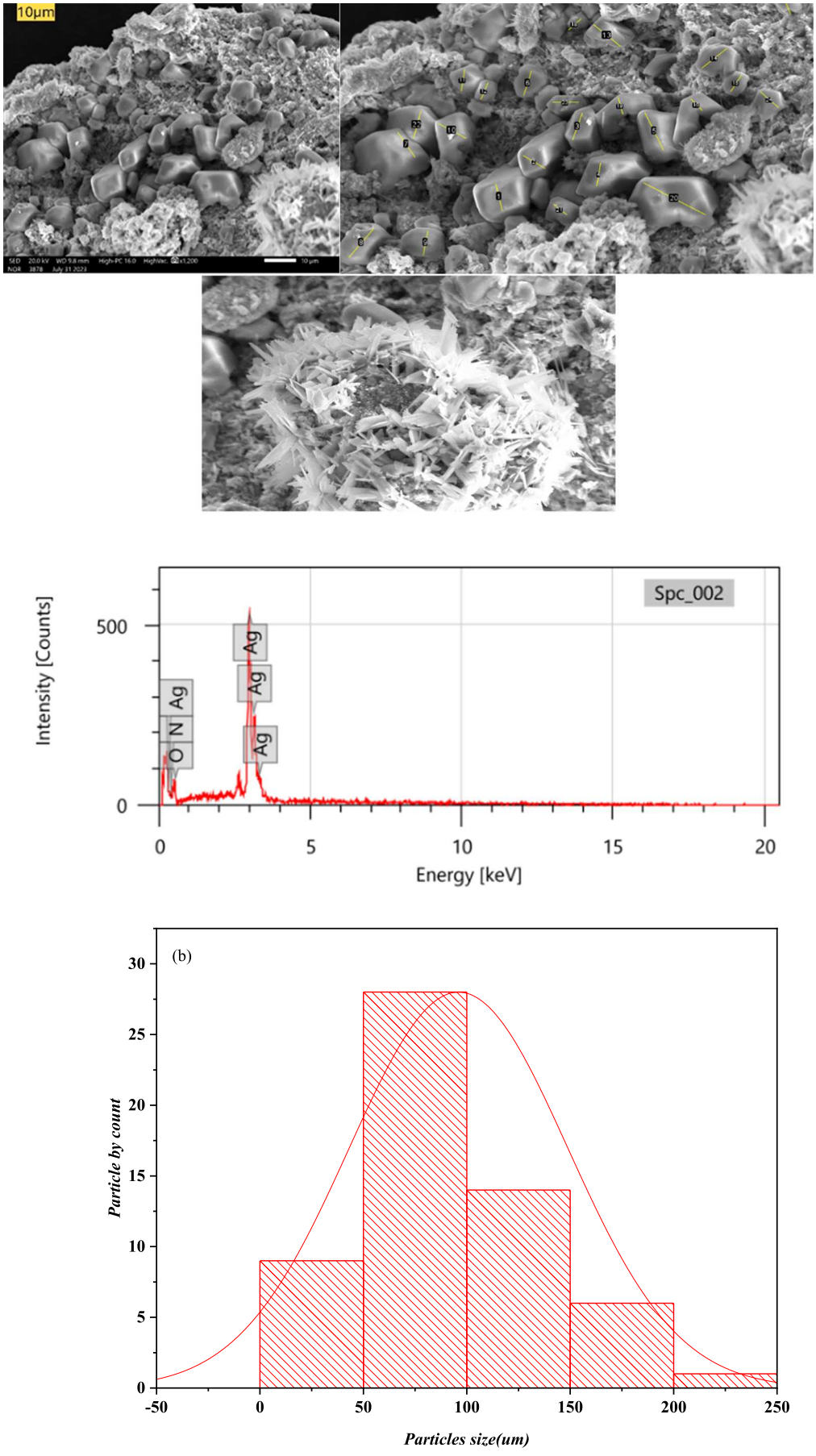


Figure 5. (a) SEM EDX analysis of the particle distribution and material composition, and (b) Particle counts of the Ag_2O NPs.

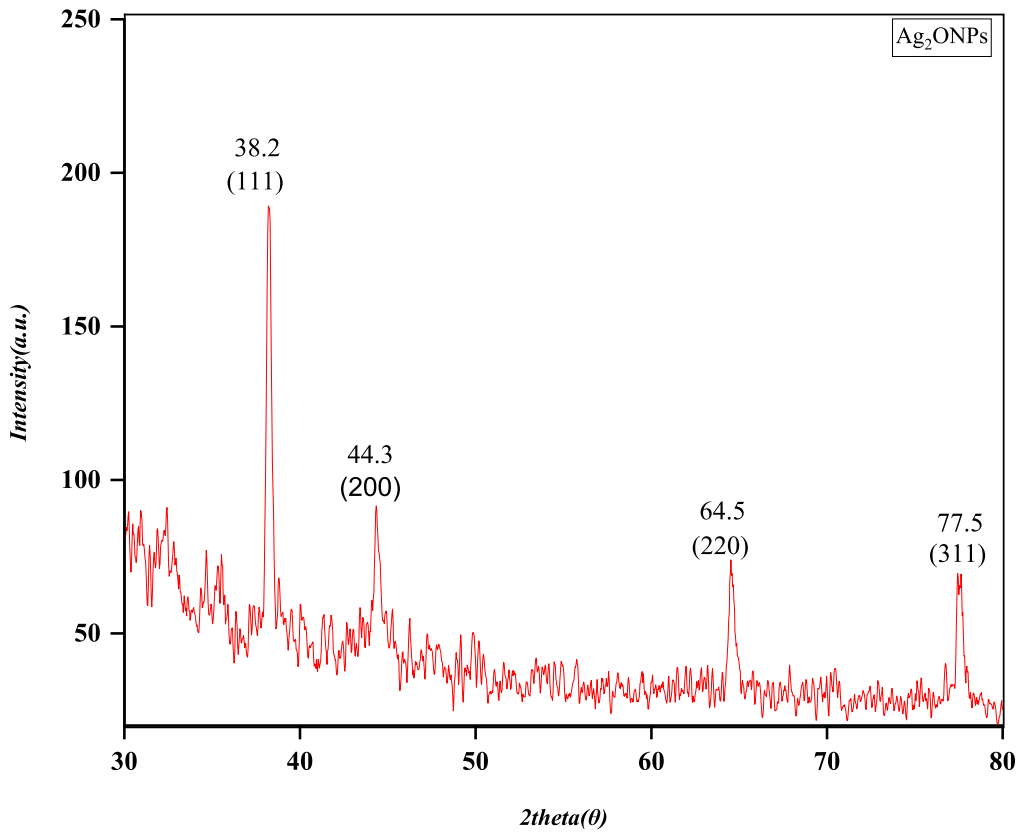


Figure 6. X-ray diffraction pattern confirming crystallinity of the Ag_2O NPs.

optimum concentration (6 mg) of Ag2O NPs (i.e., 91% degradation of the MB molecule), while concentrations greater than 6 mg led to a decrease in degradation efficiency, possibly due to the formation of agglomerated nanoparticles.

4.1. Effect of nanoparticle concentration on photocatalytic efficiency

The optimum concentration of silver oxide yeast nanoscale particles (Ag_2O NP) for efficient photo-catalysis was established by testing different concentrations ranging from 2 to 10 milligrams (mg) and observing that catalysis performance increased with increased concentration until approximately 6 mg of the nano-silver oxide, after which point further increases in concentration negatively impacted the performance of the catalyst due to clustering of the nanoparticles resulting in less available interaction areas with the photo-sensitive dye molecules as shown in figures 7(a)–(e).

A closer look at figures 7(a)–(e) reveals interesting trends regarding how nanoparticle concentration affects photocatalytic efficiency. The degradation rate was slower at a lower concentration of 2 mg, achieving approximately 70% degradation in 120 min. This can be attributed to the limited number of active nanoparticles available for dye breakdown, consistent with previous reports stating that lower catalyst dosages result in slower reaction kinetics due to reduced active sites [1]. As the concentration increased to 4 mg, the degradation rate improved significantly, reaching 91% within 120 min. This improvement is due to the increased number of active sites available for photocatalysis, which enhances the interaction between nanoparticles and dye molecules [3]. A further increase to 6 mg resulted in a similar high degradation rate, confirming that this concentration represents the optimal balance between efficiency and stability. Literature studies have also reported that silver oxide nanoparticles exhibit optimal photocatalytic activity at moderate concentrations, ensuring effective dye removal without excessive particle clustering [6].

However, at concentrations of 8 mg and 10 mg, a decline in efficiency was observed, likely due to nanoparticle agglomeration, which reduces the overall surface area available for photocatalysis. This phenomenon has been widely reported in previous studies, where excessive nanoparticle loading leads to clustering, which blocks active sites and hinders light penetration, thereby reducing photocatalytic efficiency [10]. The comparative analysis (Table S3, referred SI) confirms that concentrations of 4 mg and 6 mg best balance efficiency and stability, with degradation exceeding 85% within 120 min. These findings align with sustainable nanotechnology approaches, where resource optimization is essential. Thus, an optimal concentration of

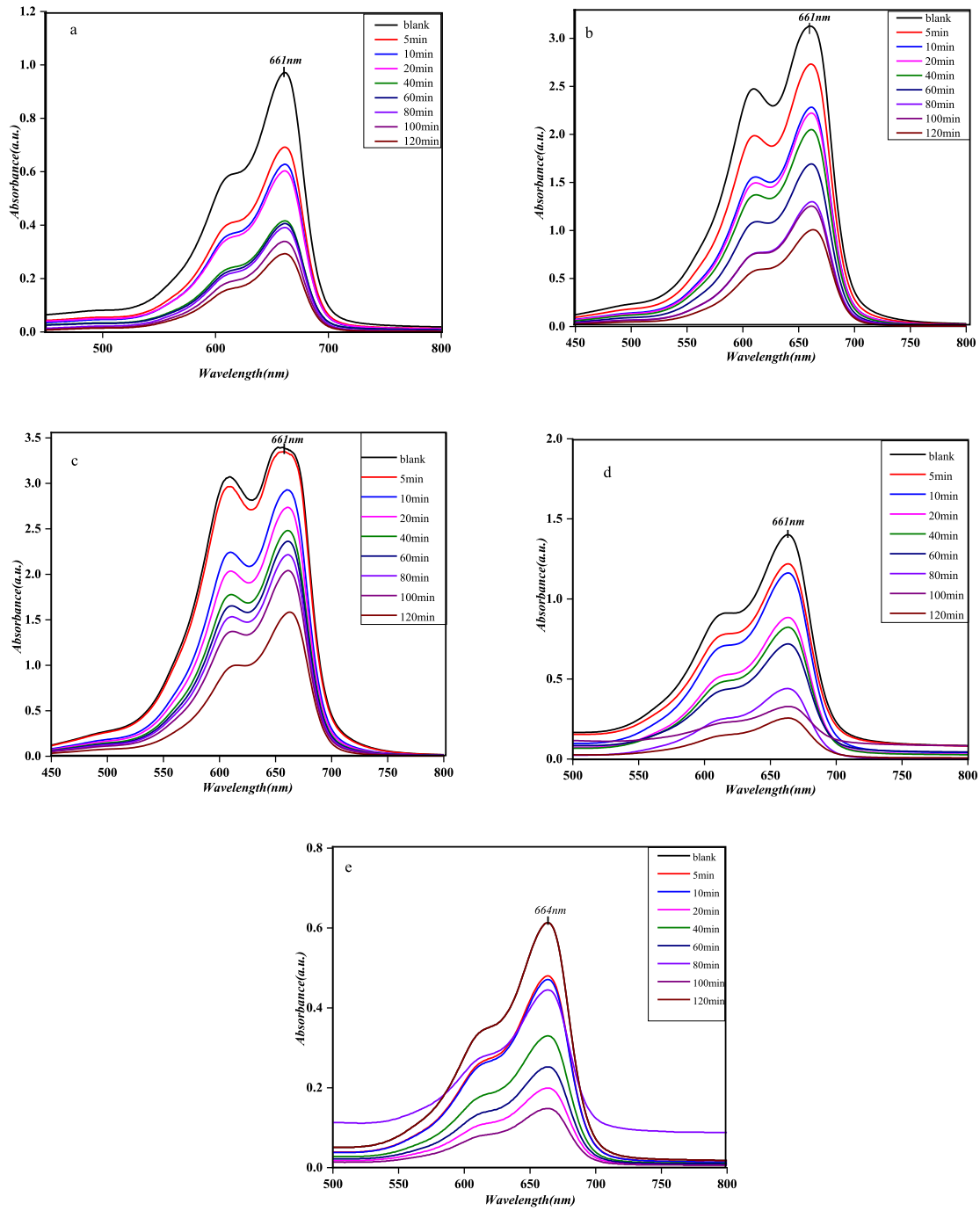


Figure 7. (a): Represents the 2 mg (b) 4 mg (c) 6 mg (d) 8 mg (e) 10 mg Ag_2O NPs in 40 ppm dye solution Values represent the mean ± standard deviation (n = 3).

4–6 mg is recommended for practical and sustainable photocatalytic applications. Later, we discussed the degradation.

4.2. Efficiency of methylene blue dye at different Ag_2O NP concentrations

Figure 8 illustrates the degradation efficiency of the methylene blue (MB) dye over 120. Minutes at varying concentrations of Ag_2O NPs (2 mg, 4 mg, 6 mg, 8 mg, and 10 mg).

Each graph (figures S2a–2e) represents the change in degradation percentage at specific time intervals, showcasing the impact of nanoparticle concentration on photocatalytic performance. The results indicate that a concentration range of 4–6 mg of Ag_2O NPs is the optimal range for achieving efficient and sustainable photocatalysis. Higher concentrations lead to aggregation, limiting further gains in degradation efficiency. These findings support the development of cost-effective strategies for environmental remediation, particularly in wastewater treatment applications.

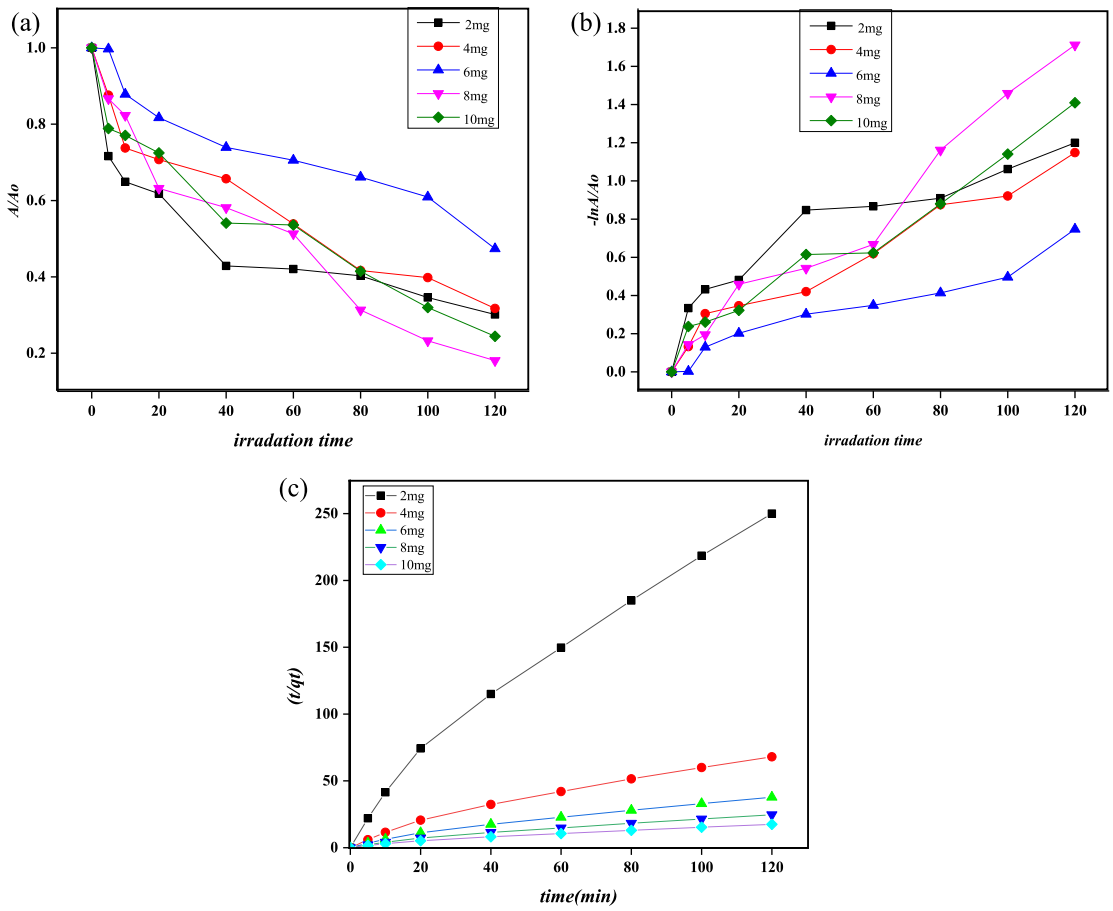


Figure 8. (a) represents the At/Ao (b) -Ln At/Ao versus irradiation time plot for pseudo-first order; (c) represents the pseudo-second order.Values represent the mean ± standard deviation (n = 3).

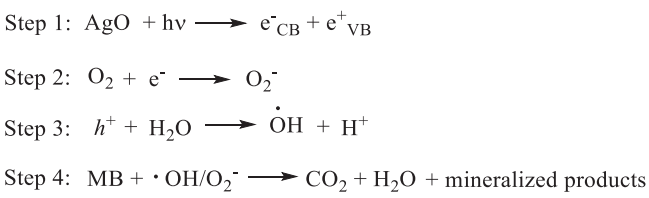


Figure 9. Proposed mechanism of photocatalytic degradation using Ag_2O nanoparticles under visible light.

4.3. Kinetic analysis of photocatalytic degradation

To gain deeper insight into the photocatalytic degradation mechanism of methylene blue (MB) using green-synthesized Ag_2O nanoparticles, both pseudo-first-order and pseudo-second-order kinetic models were evaluated. Although the 6 mg dosage of Ag_2O NPs exhibited the highest degradation efficiency (91%), the corresponding pseudo-first-order rate constant ($k_1 = 0.0053\ min^{-1}$) was lower than that of 8 mg ($k_1 = 0.0136\ min^{-1}$). However, when the data were also confirmed by the pseudo-second-order model, the 6 mg sample demonstrated the best fit with an R^2 value of 0.9821 and the highest rate constant ($k_2 = 3.29\ g{\cdot}mg^{-1}{\cdot}min^{-1}$). This indicates that the degradation process at this concentration is more accurately described by pseudo-second-order kinetics, suggesting a significant involvement of surface adsorption in addition to photocatalysis as shown in figure 10. Thus, the observed deviation in the first-order model is resolved through the improved correlation and kinetic interpretation provided by the second-order model, validating 6 mg as the optimal dosage for efficient photocatalytic activity.

4.4. Proposed mechanism for photocatalytic degradation

Furthermore, we propose a simple mechanism for the photocatalytic degradation process, as illustrated in figure 9. When Ag_2O nanoparticles are exposed to visible light, they absorb photons, which provide sufficient energy to excite electrons from the valence band to the conduction band, leaving behind positively charged

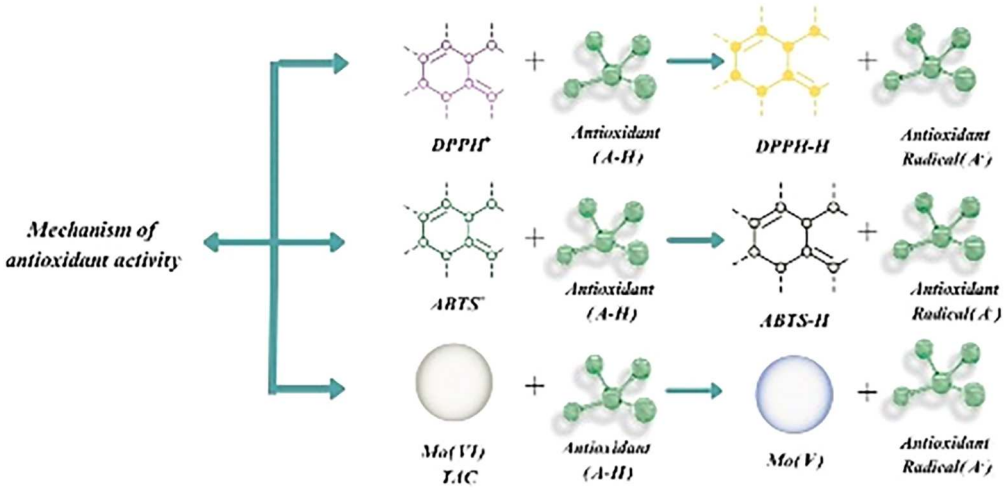


Figure 10. General mechanism of antioxidant activity (ABTS, DPPH and TAC).

holes [1]. These excited electrons interact with oxygen molecules in the solution, forming reactive oxygen species (ROS), such as superoxide anions, while the holes oxidize water molecules, generating hydroxyl radicals [3]. Both superoxide anions and hydroxyl radicals are highly reactive and play a crucial role in breaking down the dye molecules. The dye molecules undergo oxidative degradation as these reactive species attack their chemical bonds, breaking methylene blue into smaller, non-toxic components such as carbon dioxide and water [6]. However, to ensure maximum efficiency, it is essential to minimize electron–hole recombination, which can reduce the number of reactive species available for degradation. The natural capping agents from *Lobularia maritima* help stabilize the nanoparticles and prevent this recombination, making the process more efficient [10]. Studies have consistently shown that silver oxide nanoparticles demonstrate high efficiency in producing ROS under visible light, making them excellent candidates for environmental remediation [11]. This mechanism highlights how Ag_2O NPs are an effective and sustainable photocatalyst for degrading organic pollutants in wastewater treatment applications.

Overall, table S4 (as shown in the supporting file) confirms that while higher nanoparticle concentrations initially accelerate the reaction, there is a limit beyond which efficiency decreases. This finding aligns with previously reported studies that suggest an optimal photocatalyst concentration for achieving the highest degradation efficiency while preventing agglomeration-related losses. Therefore, based on these kinetic studies, a nanoparticle concentration of 4–6 mg remains the ideal for sustainable and efficient photocatalysis.

With photocatalysis proving effective in environmental applications, the study further evaluated the antioxidant properties of Ag_2O NPs, given their potential in biomedical and pharmaceutical applications.

5. Antioxidant activity

Following the evaluation of photocatalytic efficiency, the antioxidant properties of the synthesized Ag_2O NPs were assessed to explore their potential as free radical scavengers. Antioxidants play a vital role in mitigating oxidative stress, which has significant implications for both healthcare and food preservation. To thoroughly assess the antioxidant capabilities of the Ag_2O NPs, three commonly used assays were conducted: the ABTS, DPPH, and Total Antioxidant Capacity (TAC) assays. Each assay provided insights into the nanoparticles' effectiveness in neutralizing reactive species, comparable to those of known antioxidants such as ascorbic and gallic acid.

5.1. Mechanism of antioxidant activity

The antioxidant activity of nanoparticles has been assigned to the donation of electrons or hydrogen atoms from phytochemicals located on their surfaces in figure 10 The antioxidant capacity was evaluated using three different antioxidant assays: (1) The DPPH assay tests the ability of antioxidants to reduce the DPPH· free radical to its corresponding non-radical DPPH-H; (2) The ABTS assay measures the ability of antioxidants to neutralize $ABTS^{\cdot+}$ free radical cations resulting in their decolorization; (3) The TAC assay evaluates the ability of antioxidants to reduce Mo(VI) to Mo(V) creating a coloured complex that indicates total antioxidant capacity in the form of a green complex.

Table 2. Comparison with Standard Antioxidants. Values represent the mean ± standard deviation (n = 3).

SAMPLE	ABTS	DPPH	TAC	References
Ag_2O NPs	80 ± 0.02	75 ± 0.02	17.2 ± 0.01	Present work
Ascorbic acid	70 ± 0.02	85 ± 0.02	70 ± 0.01	Present work
Gallic acid	73 ± 0.02	84 ± 0.02	72 ± 0.01	Present work
Ag_2O NPs	110.36 ± 1.99	94.32 ± 1.73	74.11 ± 1.28	[29]
Ag_2O NPs	98 ± 1.6	95 ± 1.3	76.96 ± 1.57	[30]
Ag_2O NPs	—	0.70 ± 0.02	148.83 ± 2.9	[31]
Ag_2O NPs	77.63	92.88	96.72 ± 3.73	[32]

5.2. ABTS radical scavenging assay

The ABTS assay measures the ability of antioxidants to quench the ABTS radical cation, a stable blue-green chromophore that fades as the antioxidants neutralize it. The Ag_2O NPs demonstrated an antioxidant activity of 80 ± 0.02 in the ABTS assay, indicating a strong capacity to neutralize these radicals. This value suggests that the Ag_2O NPs perform comparably, and even superiorly, to ascorbic acid, which exhibited an ABTS activity of 70 ± 0.02. Given that ABTS radicals are commonly associated with oxidative stress in biological systems, these results highlight the potential application of Ag_2O NPs as effective antioxidants in biomedical fields.

5.3. DPPH free radical scavenging assay

The DPPH assay is another established method for evaluating antioxidant activity by measuring the nanoparticles' ability to quench DPPH free radicals, which are characterized by their purple color. Upon interaction with antioxidants, these radicals lose their color, indicating a reduction reaction has occurred. The Ag_2O NPs displayed a DPPH scavenging activity of 75 ± 0.02 in this assay, demonstrating robust free radical neutralization. This activity level is comparable to that of gallic acid, which has a DPPH activity of 84 ± 0.02, underscoring the effectiveness of Ag_2O NPs in capturing reactive oxygen species (ROS). Such an ability to mitigate ROS could prove valuable in applications requiring oxidative stability, such as food preservation or skincare formulations.

5.4. Total antioxidant capacity (TAC) assay

The Total Antioxidant Capacity (TAC) assay provides a holistic view of the nanoparticles' overall antioxidant potential by evaluating their capacity to quench a wide range of radicals and oxidants. In this assay, the Ag_2O NPs exhibited a TAC value of 17.2 ± 0.01, suggesting a moderate level of antioxidant capacity. While this value is lower than the TAC of standard antioxidants like ascorbic acid (70 ± 0.01) and gallic acid (72 ± 0.01), the Ag_2O NPs still demonstrated a substantial capacity for overall radical quenching. This TAC value indicates that the Ag_2O NPs have a broad antioxidant effect, which could benefit applications requiring general oxidative stability across multiple types of reactive species.

At the same time, the antioxidant activity of Ag_2O NPs was compared with that of standard antioxidants (table 2 Values represent the mean ± standard deviation (n = 3).

While the values for the ABTS and DPPH assays were comparable to or slightly lower than those of ascorbic and gallic acid, the Ag_2O NPs demonstrated a strong capacity across all assays, showcasing a balance of radical scavenging abilities. Compared to previously reported Ag_2O NPs, which showed ABTS values of up to 110.36 ± 1.99 and DPPH values of around 94.32 ± 1.73, the synthesized Ag_2O NPs offer a competitive antioxidant profile, particularly considering their green synthesis and environmentally friendly nature. Here, figure S3 illustrates the percentage scavenging activity of ABTS, DPPH, and TAC assays for the synthesized Ag_2O NPs. The results indicate that Ag_2O NPs exhibit potent antioxidant activity comparable to that of standard antioxidants, suggesting their potential applications in the biomedical and food industries as agents that mitigate oxidative stress.

The demonstrated antioxidant activity of Ag_2O NPs highlights their promise as multifunctional materials in various fields. Their ability to mitigate oxidative damage in healthcare could make them useful in antioxidant therapies and drug formulations. In the food and cosmetic industries, these nanoparticles can serve as natural stabilizers, extending shelf life by reducing oxidative degradation. Moreover, the green synthesis of Ag_2O NPs further enhances their appeal, aligning with sustainable production practices that avoid the use of toxic chemicals. The Ag_2O NPs exhibit considerable antioxidant potential, validated through ABTS, DPPH, and TAC assays. Their ability to quench radicals across various assays, combined with the environmentally friendly synthesis method, suggests that Ag_2O NPs could have extensive applications in areas prioritizing oxidative stability, ranging from food and pharmaceuticals to environmental remediation.

6. Environmental and biological implications of silver nanoparticles

Silver nanoparticles may exert certain toxic effects on microorganisms, human cells, and aquatic species due to the possible release of Ag^{+} ions. These ions can interact with cellular components and induce oxidative stress [10]. However, green-synthesized nanoparticles generally show reduced toxicity because plant-derived phytochemicals act as natural capping agents and improve biocompatibility. From an environmental perspective, Ag nanoparticles can undergo transformations such as dissolution and aggregation, which may influence their stability and ecological impact. Therefore, controlled usage, proper handling, and safe disposal practices are essential when applying Ag-based nanomaterials [33].

7. Conclusion

This study successfully demonstrated a green and sustainable approach to synthesizing silver oxide nanoparticles (Ag_2O NPs) using Lobularia maritima extract, eliminating the need for hazardous chemicals while ensuring cost-effectiveness and environmental safety. The synthesized Ag_2O NPs exhibited strong antioxidant properties, comparable to standard antioxidants, and achieved 91% photocatalytic degradation of methylene blue under visible light, making them highly effective for environmental remediation. Structural and chemical characterization confirmed their stability, crystallinity, and bioactive capping agents, supporting their potential for diverse applications. Beyond their efficacy in wastewater treatment, these Ag_2O NPs hold promise for biomedical applications, such as antimicrobial coatings and drug delivery systems. The scalability of this method makes it suitable for large-scale industrial applications, particularly in green nanotechnology and sustainable environmental management.

Acknowledgments

The authors are grateful to the Department of Chemistry at Chandigarh University and Amity University, Mohali, for providing the necessary research facilities to conduct the work related to this paper.

Data availability statement

The data is itself available in the manuscript only. No separate data is required. The data that support the findings of this study are available upon reasonable request from the authors.

Declaration of competing interest

The authors declare that they have no known competing financial interests or personal relationships that could have appeared to influence the work reported in this paper.

Author contributions

Uma Koul 0009-0004-2660-749X
Data curation (lead), Investigation (lead), Methodology (lead), Software (lead), Writing – original draft (lead)

Ruchi Bharti 0000-0001-9529-9233
Conceptualization (lead), Data curation (equal), Formal analysis (equal), Project administration (equal), Resources (lead), Supervision (lead), Validation (lead), Visualization (lead), Writing – review & editing (lead)

Renu Sharma
Formal analysis (supporting), Project administration (supporting), Resources (supporting), Supervision (supporting), Visualization (supporting), Writing – review & editing (supporting)

Ajay Thakur
Data curation (supporting), Investigation (supporting), Resources (equal), Software (equal), Validation (equal), Writing – original draft (supporting)

Monika Verma
Data curation (supporting), Formal analysis (supporting), Software (supporting), Validation (supporting), Writing – review & editing (supporting)

Annu Pandey 0000-0002-8987-8914
Conceptualization (equal), Formal analysis (equal), Methodology (equal), Project administration (equal), Supervision (equal), Writing – review & editing (equal)

References

[1] Hosseinpour-Mashkani S M and Ramezani M 2014 Silver and silver oxide nanoparticles: synthesis and characterization by thermal decomposition *Mater. Lett.* **130** 259–62
[2] Anjana V N, Joseph M, Francis S, Joseph A, Koshy E P and Mathew B 2021 Microwave-assisted green synthesis of silver nanoparticles for optical, catalytic, biological, and electrochemical applications *Artif Cells Nanomed Biotechnol.* **49** 438–49
[3] Sharma R K, Yadav S, Dutta S, Kale H B, Warkad I R and Zbořil R 2021 Silver nanomaterials: synthesis and (electro/photo) catalytic applications *Chem. Soc. Rev.* **50** 11293–380
[4] Abd El-Hack M E, El-Saadony M T, Shafi M E, Zabermawi N M, Arif M and Batiha G E 2020 Antimicrobial and antioxidant properties of chitosan and its derivatives and their applications: a review *Int. J. Biol. Macromol.* **164** 2726–44
[5] Paladini F and Pollini M 2019 Antimicrobial silver nanoparticles for wound healing application: progress and future trends *Materials (Basel)* **12** 2540
[6] Pryshchepa O, Pomastowski P and Buszewski B 2020 Silver nanoparticles: synthesis, investigation techniques, and properties *Adv. Colloid Interface Sci.* **284** 102246
[7] Villaverde-Cantizano G, Laurenti M, Rubio-Retama J and Contreras-Cáceres R 2021 Reducing agents in colloidal nanoparticle synthesis–an introduction *Colloids Surf A Physicochem Eng Asp.* **610** 125680
[8] Jiang Z, Li L, Huang H, He W and Ming W 2022 Progress in laser ablation and biological synthesis processes: 'top-down' and 'bottom-up' approaches for the green synthesis of Au/Ag nanoparticles *Int. J. Mol. Sci.* **23** 14658
[9] Hegab H, Shaban I, Jamil M and Khanna N 2023 Toward sustainable future: strategies, indicators, and challenges for implementing sustainable production systems *Sustain. Mater. Technol.* **36** e00617
[10] Taghavizadeh Yazdi M E, Amiri M S, Akbari S, Sharifalhoseini M, Nourbakhsh F, Mashreghi M, EhsanYousefi, Abbasi M R, Modarres M and Es-haghi A 2020 Green synthesis of silver nanoparticles using helichrysum graveolens for biomedical applications and wastewater treatment *BioNanoScience* **10** 1121–7
[11] Jagadeeswar V, Dhinesh V, Roopan S M and Samuel E J J 2023 Plant extract-mediated synthesis of Ag-doped ZnO: eco-friendly nanomaterial for environmental restoration, microbial inhibition, cell toxicity, antioxidant potential, and sensing *Colloid J.* **85** 827–45
[12] Singh H, Desimone M F, Pandya S, Jasani S, George N and Adnan M 2023 Revisiting the green synthesis of nanoparticles: uncovering influences of plant extracts as reducing agents for enhanced synthesis efficiency and its biomedical applications *Int. J. Nanomedicine* **18** 4727–50
[13] Villagrán Z, Anaya-Esparza L M, Velázquez-Carriles C A, Silva-Jara J M, Ruvalcaba-Gómez J M and Aurora-Vigo E F 2024 Plant-based extracts as reducing, capping, and stabilizing agents for the green synthesis of inorganic nanoparticles *Resources* **13** 70
[14] Ullah Z, Gul F, Iqbal J, Abbasi B A, Kanwal S, Chalgham W, El-Sheikh M A, Diltemiz S E and Mahmood T 2023 Biogenic synthesis of multifunctional silver oxide nanoparticles (Ag2ONPs) using Parieteria alsinaefolia delile aqueous extract and assessment of their diverse biological applications *Microorganisms* **11** 1069
[15] Masho T J, Ayane M M, Endale G N, Adula S H, Negasa Y D, Likasa B W, Mudda T S, Negari G K, Amante H C and Jida S M 2025 Biosynthesis, characterization of Ag_2O nanoparticles for enhancement of antioxidant and photo degradation activities *Results in Chemistry* **13** 101919
[16] Gungure A S, Jule L T, Nagaprasad N and Ramaswamy K 2024 Studying the properties of green synthesized silver oxide nanoparticles in the application of organic dye degradation under visible light *Sci. Rep.* **14** 26967
[17] Verma C, Chauhan D S, Aslam R, Banerjee P, Aslam J and Quadri T W 2024 Principles and theories of green chemistry for corrosion science and engineering: design and application *Green Chem.* **26** 4270–357
[18] Gong X, Jadhav N D, Lonikar V V, Kulkarni A N, Zhang H and Sankapal B R 2023 An overview of green synthesized silver nanoparticles towards bioactive antibacterial, antimicrobial and antifungal applications *Adv. Colloid Interface Sci.* 103053
[19] El Messaoudi N, Ciğeroğlu Z, Şenol Z M, Kazan-Kaya E S, Fernine Y and Gubernat S 2024 Green synthesis of $CuFe_2O_4$ nanoparticles from bioresource extracts and their applications in different areas: a review *Biomass Convers. Biorefin.* 1–22
[20] Gupta D, Boora A, Thakur A and Gupta T K 2024 Green and sustainable synthesis of nanomaterials: recent advancements and limitations *Environ. Res.* **231** 116316
[21] Singh R, Thakur P, Thakur A, Kumar H, Chawla P and Rohit J V 2021 Colorimetric sensing approaches of surface-modified gold and silver nanoparticles for detection of residual pesticides: a review *Int. J. Environ. Anal. Chem.* **101** 3006–22
[22] Thakur A, Verma M, Bharti R and Sharma R 2023 Recent advancement in the green synthesis of silver nanoparticles *Curr. Chin. Sci.* **3** 322–48
[23] Thakur A, Verma M, Setia P, Bharti R, Sharma R and Sharma 2023 DFT analysis and *in vitro* studies of isoxazole derivatives as potent antioxidant and antibacterial agents synthesized via one-pot methodology *Res. Chem. Intermed.* **49** 859–83
[24] Verma M, Thakur A, Kapil S, Sharma R, Sharma A and Bharti R 2023 Antibacterial and antioxidant assays of novel heteroaryl-substituted methane derivatives synthesized via a ceric ammonium nitrate (CAN)-catalyzed one-pot green approach *Mol Divers* **27** 889–900
[25] Thakur A, Bharti R, Verma M, Sharma R, Sharma A and Gupta A 2023 Ultra-sonicated one-pot synthesis of potent bioactive biscoumarin and polycyclic pyranodichromenone scaffolds in aqueous media: a complementary tool to organic synthesis *Synthesis (Stuttg)* **55** 3129–44
[26] Prakash R, Bharti R, Thakur A, Verma M and Sharma R 2025 Environmentally benign green approach for the synthesis of IONPs using Vicia faba fruit extract and their antioxidant activities *Sustain. Chem. Eng.* **6** 1–113
[27] Goudjil M B, Ladjel S, Zighmi S, Hamada D, Mahcene Z and Bencheikh S E 2025 Green biosynthesis of Ag2O nanoparticles by aqueous leaves extract of Thymus capitatus (Lamiaceae): effect of silver nitrate weight in optical and their biological activity *Inorganic and Nano-Metal Chemistry* **55** 839–50
[28] Jabeen S, Qureshi R, Ikram M, Omar A A, Hussain M and Elnaggar 2023 Phyto-fabrication and characterization of silver nanoparticles using Withania somnifera: investigating antioxidant potential *Green Process Synth.* **12** 20230167
[29] Vrushabendrakumar D, Rajashekhar H, Riddell S, Kalra A P, Alam K M and Shankar K 2021 Synthesis, characterization, and visible light photocatalytic activity of solution-processed free-standing 2D Bi2O2Se nanosheets *Nanotechnology* **32** 485602

[30] Jan H, Zaman G, Usman H, Ansir R, Drouet S and Gigliolo-Guivarc'h N 2021 Biogenically proficient synthesis and characterization of silver nanoparticles (Ag-NPs) employing aqueous extract of Aquilegia pubiflora along with their *in vitro* antimicrobial, anti-cancer and other biological applications *J. Mater. Res. Technol.* **15** 950–68
[31] Das B, De A, Podder S, Das S, Ghosh C K and Samanta A 2021 Green biosynthesis of silver nanoparticles using Dregea volubilis flowers: characterization and evaluation of antioxidant, antidiabetic and antibacterial activity *Inorg. Nano-Met. Chem.* **51** 1066–79
[32] Yarrappagaari S *et al* 2022 Eco-friendly synthesis of silver nanoparticles from the whole plant of Cleome viscosa and evaluation of their characterization, antibacterial, antioxidant, and antidiabetic properties *Saudi J. Biol. Sci.* **27** 3601–14
[33] Rahimi E, Asefi F, Afzalinia A, Khezri S, Zare-Zardini H, Ghorani-Azam A, Es-haghi A and Yazdi M E 2023 Chitosan coated copper/silver oxide nanoparticles as carriers of breast anticancer drug: cyclin D1/P53 expressions and cytotoxicity studies *Inorg. Chem. Commun.* 111581